# Experimental investigation of the mechanical micro structural and thermal properties of thin CrAIN layers deposited by PVD technique for various aluminum percentages.

T. Ghrib[a,*] , B. Tlili[b], C. Nouveau[c],Y. Benlatreche[c], M. Lambertin[c], N. Yacoubi[a], M. Ennasri[b]

[a]*Photothermal Laboratory, I PEI 8000 Nabeul, Tunisia.*
[b]*UR. Mécanique Appliquée, Ingénierie et Industrialisation (M.A21), ENIT, BP 37 Le belvédère 1002 Tunis, Tunisie*
[c]*Laboratoire Bourguignon des Matériaux et Procédés (LaboMap), CER ENSAM de Cluny 71250, France*

**Abstract**

The thin film of chromium nitride and their derivatives obtained by the filing process physical vapour deposition attract more and more attention from industry given their high resistance to wear. This quality of these coatings may be linked to their good mechanical and tribological properties.
Several experimental investigations have led to the development of CrAlN (Chronium Aluminum Nitride) hard coatings by varying the aluminium target bias voltage, in preference to the traditional CrN coating.
The present work is based on the investigation of physical and mechanical properties of CrAlN coating deposited on a silicon substrate and the effect of the aluminium proportion on their variation.
The results demonstrate that variation in aluminum proportion alters the resulting columnar morphology, porosity and the thermal properties. The correlation between aluminum proportions in CrAlN coatings and his thermal properties revealed that the conductivity and the diffusivity are influenced primarily by size and shape distribution of the pores and secondarily by decrease of the stitch parameter dimension.

Keywords :CrAlN, PVD, thermal properties, thin films, PTD technique.

## 1. Introduction

Since the last decade we observe an increasing interest for studying surfaces for their essential role to exert a decisive influence on diverse characteristics as well as corrosion, catalyses, friction (wear, lubrication...), adherence, sintering, etc.

* *E-mail address*: taher.ghrib@yahoo.fr

The purpose of the physical vapor deposition (PVD) process is to protect the surface steel from corrosion and wear and then decrease their reactivity with the external medium. The deposition of a CrxN [1] layer on the steel surfaces will modify greatly its physical properties such as hardness and thermal properties, its resistance in fretting is remarkable and until today it is difficult to measure it due to their low Thickness.

In presence of oxygen gas the CrxN will favor the formation a Cr2O3 layers which has a good protection against adhesive wear and corrosion and improves the resistance to oxidation (<800 ° C), compared with TiN coatings and TiC (<500 ° C) [2, 3]. For this reason CrN layers are used in the past for cutting metal alloys non-ferrous and plastic process [4].

The CrAlN represent a new generation of coating based on the chromium alloy which was investigated considerably by many authors [5-7]. The addition of aluminum will affects the structure of coating and then the Young modulus values which is related to the content of aluminum.

In this paper, we will investigate the mechanical, micro-structural, and thermal proprieties of the CrAlN coatings.

## 2. Preparation of the sample

The thin layer of CrAlN is filed on silicon platelets, using a magnetron sputtering mode DC from two targets of high purity. The backings were mounted on a continuously rotating planetary holder inside the vacuum chamber. The atmosphere was chosen in order to produce a CrAlN layer. The deposition conditions such as target power, bias voltage, temperature, rotational velocity and deposition time are illustrated in table 1.

Table1. Deposition conditions.

| Unit | Target power (kW) | Biasing (V) | | Rotation velocity (rpm) | Time (min) | Gas pressure (mbar) | |
|---|---|---|---|---|---|---|---|
| | | Al | Cr | | | Ar (80%) | $N_2$ (20%) |
| CrN<br>CrAlN | 4 | 0<br>-300<br>-500<br>-700<br>-900 | -900 | 0.5 | 90 | $4.10^{-3}$ | $4.10^{-3}$ |

Nitrogen of very high purity was introduced into the vacuum chamber. The pressure in the deposition chamber was $10^{-6}$ mbar. The distance between the target and surface backing was 10 cm. Previous the deposition operation, the surface backings and targets were further cleaned by argon ion bombardment.

The influence of the aluminum biasing target on the microstructure and the thermal properties is investigated.

## 3. Micro-structural characterization and morphological

The growth of the layer begins with the arrival of aluminum and chromium atoms undergoing the formation of small islands matter from nucleation.

Hones [7] schematized this process of deposit as the growth of columns which take the shape of cones of various diameters. For the first atomic layers (low thicknesses of the deposit), we are in presence of closer columns relatively identical and stuck, who causes its progressive thickening (Fig1.a). This observation by SEM on a cross-section shows that the columns are perpendicular at the backing surface (Fig1.b) which is in agreement with the Thornton model [8].

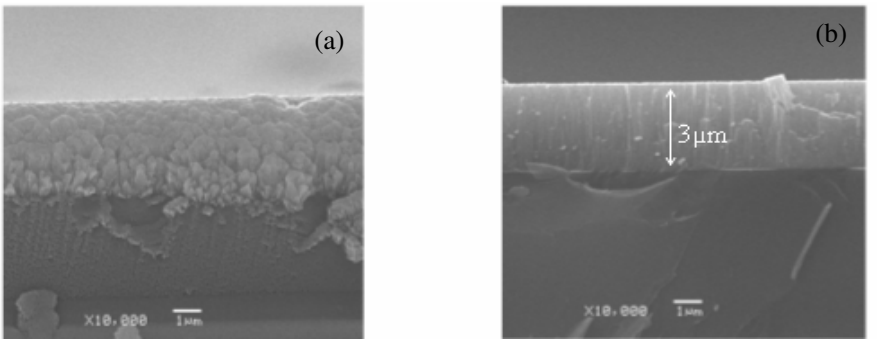


Fig 1: 1.a: Scanning electron micrograph of CrAlN layer in the state of growth;
1.b: Scanning electron micrograph of CrAlN transversal section layer made by fractography

The EDS analysis of the samples shows that the atomic percentages depends on the biasing of aluminum and chromium target and remain constant for higher absolute values as shown on Fig 2.

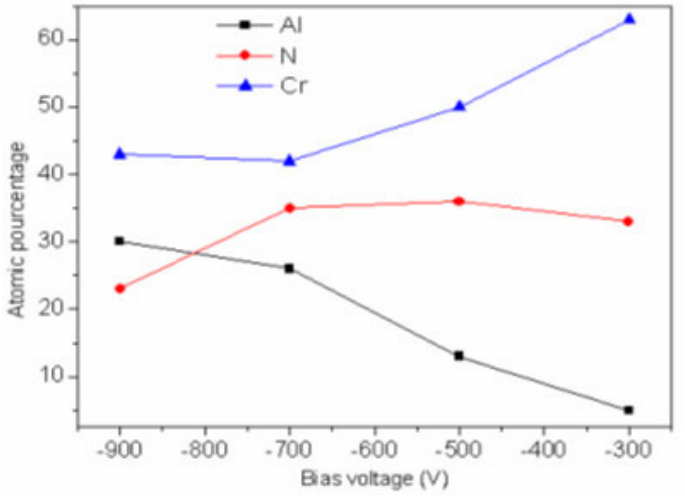


Fig 2: Atomic percentage evolution with biasing aluminum target.

Using the diffraction RX, the structure and the crystallographic orientation of these deposited CrAlN coatings on a platelets of silicon (100) shows the presence of a reflection peak corresponding to the stripe (200) [9], which is become more and more great when the bias voltage increases (Fig 3). The (111) peak of CrN appear clearly at 13% of aluminium and disappear at 28%. This proves that the layers are formed by crystallization up to 28%Al proportion corresponding to 700V bias voltage.

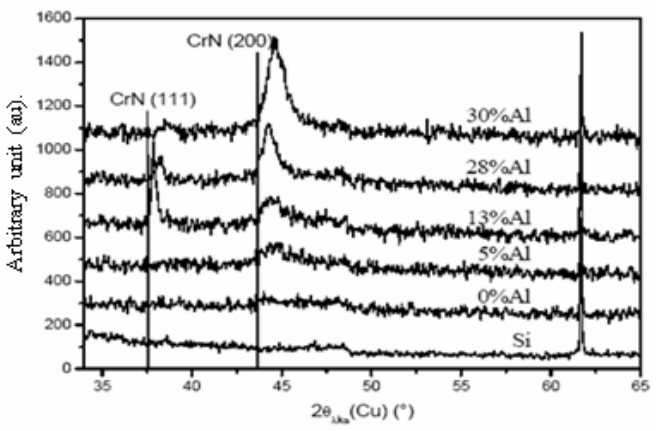


Fig.3: Spectra obtained by x-rays for CrAlN coatings with differents aluminium percentage.

In order to visualize the surface topography of the CrAlN coatings we used the atomic force microscopy (AFM), we have observed the presence of some domes with a very small scale who are scattered on the surface and whose dimensions increase with the bias voltage (Fig 4).

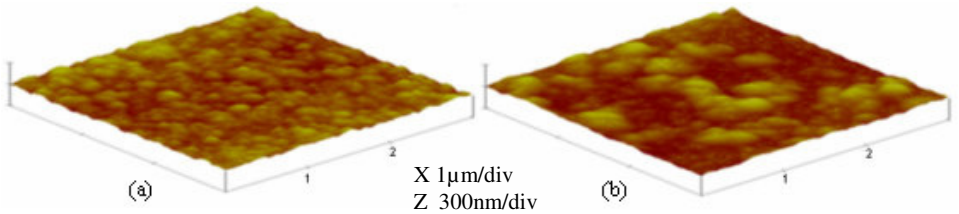


Fig.4: Topography of CrAlN surface layers for -500 V (a) and - 900 V. (b).

## 4. Mechanical properties of deposited layers

### *4.1. Residual stress*

The residual stress was determined using the Newton method (1642-1727). This method is based on the principle to Stoney theory [10]. If we consider that the stress is isotropic in the plane of the substrate, the film produced is a portion of a sphere of radius R, then the constraint is expressed by the following formula:

$$\sigma = \pm \frac{E_s}{(1-\nu_s)} \times \frac{e^2_s}{e_f}\left(\frac{1}{R} - \frac{1}{R_0}\right) \quad (1)$$

where, Es: Young's modulus of substrate, vs: Poisson's ratio of substrate, es: Thikness of substrate, ef : Thickness of the film,R0: radius of curvature before deposition, R: radius of curvature after deposition, And knowing this parameter we deduce the residual stress. Fig. 5 shows that is vary for this samples from 1,1 to 3,6 GPa. Compulsion decreases with the increase in the proportion of aluminium in the CrAlN film to be stabilized between the proportions 5 and 30%, and then it increases again, reaching the value of 3.6 GPa. This is explained primarily by the

formation of a structures columnar, which is less dense and therefore less stresses than the amorphous structure. The increase in the residual stress is associated with the substitution of chromium atoms with aluminium than we can deduce that the adherence of the CrAlN layer became very important for aluminium proportions higher than 28%.

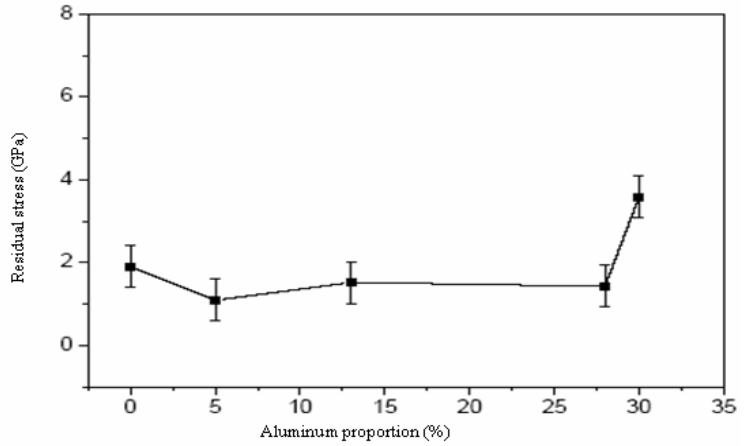


Fig.5: Residual stresses versus aluminum proportion in the CrAlN layers.

*4.2. Micro-hardness*

As presented in fig. 6 work the micro-hardness and Young modulus are very important, they present a curve similar to that of residual stresses as the micro-hardness varies from 23 to 36 GPa and the Young modulus varies from 380 to 460 GPa and present both a maximum for a percentage of 28% Aluminum. This results show the possibility to ameliorate of mechanical properties metallic materials on covering them with a CrAlN layer.

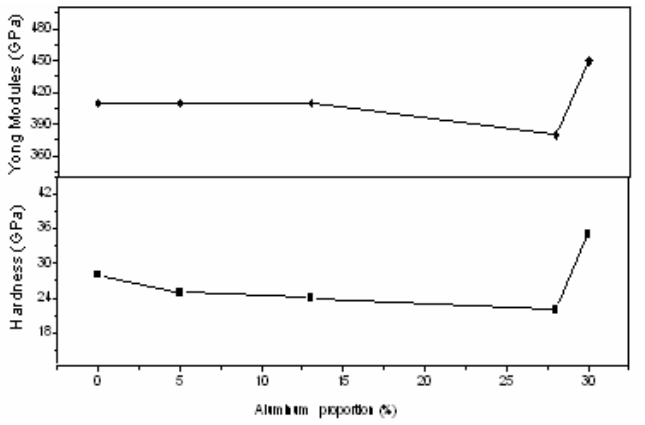


Fig.6: Hardness and Young modulus variation with Al proportion in CrAlN films.

## 5. Thermal properties

The photothermal properties are determined by the photothermal deflection technique (PTD) [11].

### *5.1. Theoretical model*

The photothermal deflection technique (PTD) consists to heat a sample with a periodically pump beam (Fig. 7), the warmth absorbed who diffuses in the surrounding fluid producing a refractive index gradient. A probe beam skimming the surface sample and passes into the refractive index gradient zone undergo a deflection ψ. This deflection is related to the surface temperature then to the thermal properties of the sample and various neighboring media.

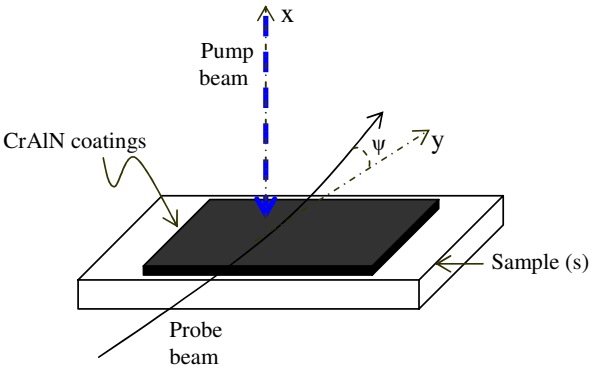


Fig.7: Schematic representation of the probe beam deflection.

The CrAlN coating is deposited on a (100) silicon substrate whose thermal properties are known. The probe beam deflection is deduced by writing the heat equation in the all media and using the beam radius equation in inhomogeneous refractive index medium [11]. So we obtain the following expression

$$\psi = |\psi| e^{j(\omega t+\varphi)} = \frac{\sqrt{2}\, l}{n\, \mu_f} \frac{dn}{dT_f} |T_0| e^{-\frac{x}{\mu_f}} e^{j(\theta+\frac{5\pi}{4}-\frac{x}{\mu_f})} e^{j\omega t} \qquad (2)$$

where $T_0$ the temperature at the surface [11-13].

$$T_0 = E[(1-b)e^{-\sigma_s l_s}[(1-r)(1-c)e^{\sigma_c l_c} + (1+r)(1+c)e^{-\sigma_c l_c} - 2(1+r\,c)e^{-\alpha l_c}] - (1+b)e^{\sigma_s l_s}[(1-r)(1+c)e^{\sigma_c l_c} + (1+r)(1-c)e^{-\sigma_c l_c} - 2(1-r\,c)e^{-\alpha l_c}]] / [[(1+b)e^{\sigma_s l_s}[(1+g)(1+c)e^{\sigma_c l_c} + (1-g)(1-c)e^{-\sigma_c l_c}] - (1-b)e^{-\sigma_s l_s}[(1+g)(1-c)e^{\sigma_c l_c} + (1-g)(1+c)e^{-\sigma_c l_c}]] \qquad (3)$$

$$b = \frac{K_b}{K_s}\sqrt{\frac{D_s}{D_b}},\ c = \frac{K_c}{K_s}\sqrt{\frac{D_s}{D_c}},\ g = \frac{K_f}{K_c}\sqrt{\frac{D_c}{D_f}},\ r = \frac{(1-j)\alpha}{2\mu_c},\ \sigma_i = (1+j)\sqrt{\frac{\pi f}{D_i}}$$

$K_i$, $D_i$, and $\mu_i$ are respectively the thermal conductivity, the thermal diffusivity and the thermal length of the i (f, c, s, b) medium, designating the fluid as 'f', the black graphite layer as 'c', the substrate as 's' and the backing 'b'.

$$|\psi| = \frac{\sqrt{2}\,L}{n\,\mu_f}\frac{dn}{dT_f}|T_0|e^{-\frac{x}{\mu_f}} \qquad (4a)$$

$$\varphi = -\frac{x}{\mu_f} + \theta + \frac{5\pi}{4} \qquad (4b)$$

$|\psi|$ and $\varphi$ are respectively the amplitude and phase of the probe beam deflection. $|T_0|$ and θ are respectively the amplitude and phase of the sample's surface temperature.

*5.2. Experimental set-up*

The experimental set-up shown on Fig. 8 is described in detail in ref [12]; it is composed with a halogen heating lamp, a laser probe beam, a photodetector position sensor and a look-in amplifier. The light coming from the halogen lamp is modulated by a mechanical chopper. The sample is fixed on a table improving micrometric displacement. A laser probe beam skimming the sample surface is deflected. Its deflection is measured by a position photodetector sensor.

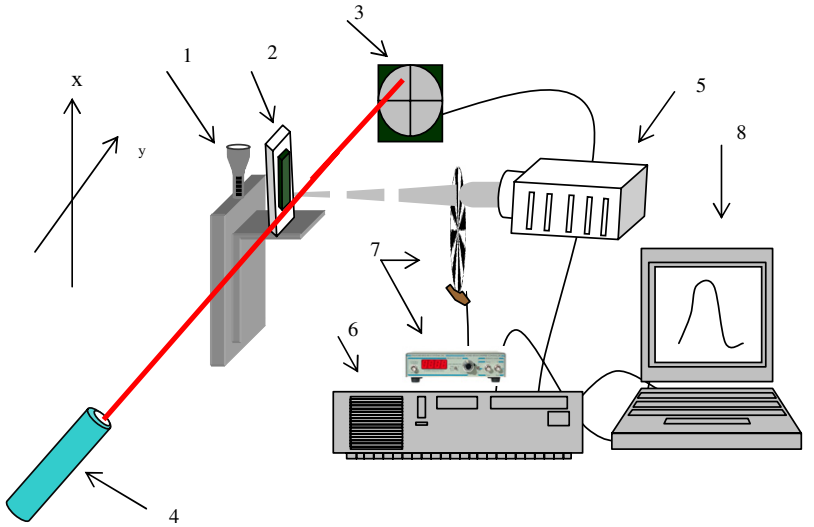


Fig.8: 1-Table of horizontal and vertical micrometric displacement, 2-Sample, 3- Photodetector , 4- He-Ne Laser probe beam, 5-halogen Lamp, 6-look-in amplifier, 7-Mechanical Chopper, 8-PC.

*5.3. Experimental results*

In order to determine the thermal properties of the CrAlN coatings we have plotted on Fig. 9 the experimental variation of phase and normalized amplitude of the PTD signal versus the square root modulation frequency. The difference between these curves is attributed to the difference of their thermal conductivity and thermal diffusivity. Using the theoretical model presented in section 4.1, one can deduce the couple thermal conductivity-thermal diffusivity ($K_s$, $D_s$). The coincidence between experimental and theoretical curves is obtained for a known and unique value of $K_s$ and $D_s$ [12,13].

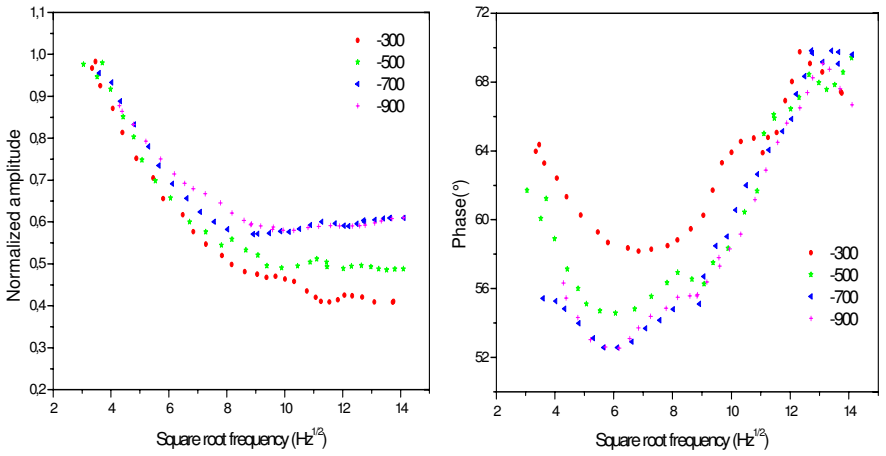


Fig.9: Photothermal signal normalized amplitude and phase evolution with square root modulation frequency of the deposited CrAlN layer for various biasing voltage.

On Fig. 10 are plotted the thermal conductivity and the thermal diffusivity variation versus the bias. The conductivity and thermal diffusivity of CrAlN coatings decrease gradually if the aluminium proportion in the layers increases (bias voltage increases in absolute value), to move towards a stabilizing values of 2,8 $W.m^{-1}.K^{-1}$ for the thermal conductivity and $5\times10^{-7}$ $m^2.s^{-1}$ for the thermal diffusivity. The thermal properties became constant for a percentage of aluminium higher than 28% (bias < -700V) which may be explained by a stabilisation of the crystalline structure.

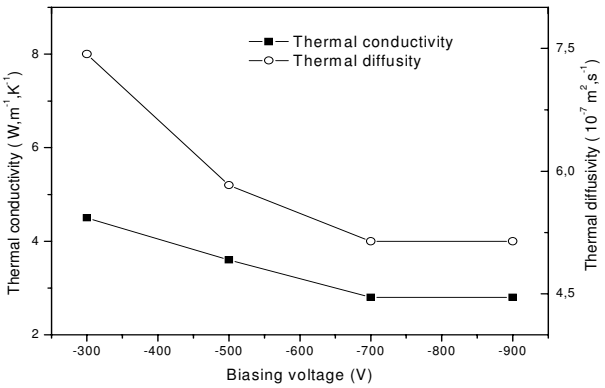


Fig.10: Thermal properties change compared to the bias voltage.

We interpret the decrease of the thermal conductivity with the aluminum proportion by the decreases of the phonons mean free path λ. As the phonon is considered like quasi – particles which obey to the kinetic theory of gases, then the thermal conductivity is bound to the phonons mean free path λ by the following relationship [14]:

$$K = \frac{\rho c v}{3}\lambda \qquad (4)$$

where ν is the mean speed of the particles of a diluted gas at the room temperature which value is $v = 3500 m.s^{-1}$.

Moreover, the report between the conductivity and thermal diffusivity, will give the volumic specific heat (ρc) which is inversely proportional to the porosity and the latter evolution based on the proportion of aluminium in CrAlN layers which gives an idea on evaluating the desired porous films (Fig. 11).

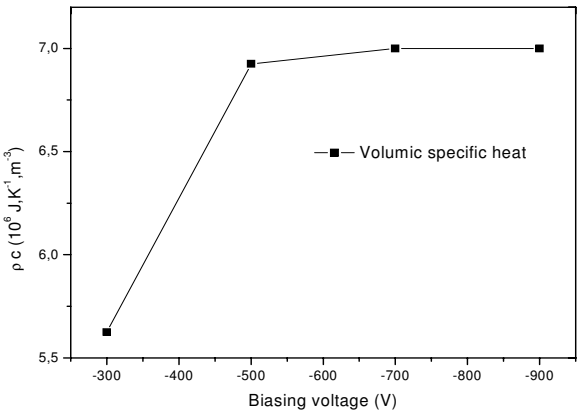


Fig. 11: Volumic specific heat evolution with the biasing voltage.

We notice that volumic specific heat depend on the aluminium bias voltages target. In fact the volumic specific heat increases versus the bias voltage and stabilizes for the extreme and stabilizes for a voltage below -600 for about 20%Al which provides low porosity.

Hence, when the aluminum proportion increases to the benefit of Cr one in CrAlN layers, and since the radius of the aluminum atoms are lower than those of Crome we can say that the porosity will decrease.

## Conclusion

The results presented in this paper show clearly the influence of the aluminum proportion of the CrAlN layer on the stoechiometry, the adherence, the Young modulus and the micro-hardness whose became very important for a proportion of aluminium higher than 28% and improves the layer adherence with the substrate.

In addition the increase in aluminium percentage on the CrAlN layer decreases these thermal properties gradually, until reaching values of stabilization for 28% and 30% of aluminium proportion. Thereafter, with direction meadows, the volumic specific heat shows that the porosity of the CrAlN layers decreases by increasing aluminum proportion which stabilizes for a proportion of aluminum about 20%.

## References

[1] M. Uchida, N. Nihira, A. Mitsuo, K. Toyoda, K. Kubota, T. Aizawa, Surface and Coatings Technology 177 –178 (2004) 627–630.
[2] C. Friedrich, G. Berg, E. Broszeit, C. Berger, Materialwissenschaften und Werkstofftechnik 28 (1997) 59-76.
[3] O. Knotek, W. Bosch, M. Atzor, W.-D. Münz, D. Hoffmann, J. Goebel, High Temperature-High Pressures 18 (1986) 435-442.
[4] S. Hofmann, H.A. Jehn, Werkstoffe und Korrosion 41 (1990) 756-760.
[5] J. Vetter, E. Lugscheider, S.S. Guerreiro, Surface and Coatings Technology 98 (1998) 1233-1239.
[6] E. Lugscheider, K. Bobzin, K. Lackner, Surface and Coatings Technology 174 –175 (2003) 681–686.
[7] P. Hones, R. Consiglio, N. Randall, F. Levy, Surf. Coat. Technol. 125 (2000)179
[8] J.A. Thornton, J. Vac. Sci. Technol. 11 (1974) 666-670

[9] I. Safi, Surface and Coatings Technology 127 (2000) 203-218.
[10] Q. Wang, H. Ishikawa, S. Nakano , H. Ogiso, J. Akedo, Vacuum 75 (2004) 225–229.
[11] A.C. Boccara, D. Fournier, J. Badoz, App. Phys. Lett. 36 (1980) 130-132.
[12] T. Ghrib, N. Yacoubi, F. Saadallah, Sensors and Actuators A135 (2007) 346–354.
[13] T. Ghrib, F. Bejaoui, A. Hamdi, N. Yacoubi, Thermochimica Acta 473 (2008) 86-91.
[14] X.J. Liu, Q.J. Huang, S.Y. Zhang, A.H. Luo, C.X. Zhao, Journal of Physics and Chemistry of Solids 65 (2004) 1247–1251.